

The First Photocrystallographic Evidence for Light-Induced Metastable Linkage Isomers of Ruthenium Sulfur Dioxide Complexes

Andrey Yu. Kovalevsky,[†] Kimberly A. Bagley,[‡] and Philip Coppens^{*†}

Contribution from Chemistry Department, State University of New York at Buffalo, Buffalo, New York 14260, and Department of Chemistry, State University College of New York at Buffalo, Buffalo, New York, 14222

Received February 27, 2002

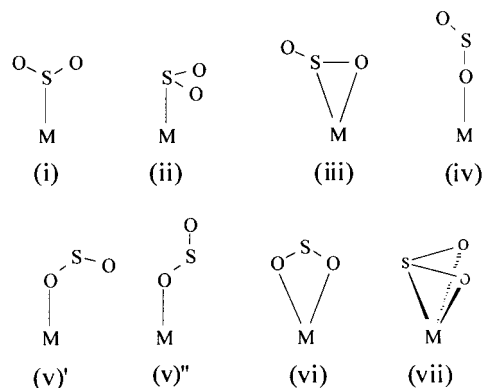
Abstract: Light-induced metastable linkage isomers of *trans*-[Ru(NH₃)₄Cl(SO₂)]Cl and *trans*-[Ru(NH₃)₄(H₂O)(SO₂)](C₆H₅SO₃)₂ have been identified for the first time using photocrystallographic methods. In both linkage isomers the SO₂ ligand is side bound, but the Ru–O and Ru–S distances are considerably longer and almost equal in the *trans*-H₂O isomer. DFT calculations confirm that both isomers correspond to minima on the ground-state potential energy surface and also predict the existence of a second oxygen-bound isomer for both compounds. The decay of the light-induced species has been studied by both DSC and IR. Activation energies for the thermal back-reaction, as derived from the temperature-dependent disappearance of light-induced IR bands, are 50.0 and 58.4 kJ/mol for the two isomers, which is larger than the corresponding numbers for photoinduced side-bound nitrosyl linkage isomers.

Introduction

The combination of crystallographic and spectroscopic techniques in a single experiment makes it possible to study light-induced changes in crystals, from the generation of long-lived metastable states to the creation of very short-lived transient states. In a *photocrystallographic* experiment a diffractometer-mounted crystal is irradiated with exciting light, either prior to or during collection of the diffraction pattern. We have used the method to study photoinduced metastable states of nitrosyl and dinitrogen compounds^{1,2} and have recently reported a time-resolved stroboscopic study of the 50 μs lifetime excited state of a diplatinum complex.³ We describe here the first photocrystallographic study of linkage isomerism in transition metal SO₂ complexes.

Sulfur dioxide is a well-known example of an extremely versatile ligand.^{4,5} It can form a variety of coordination complexes with most of the transition metals. Depending on the nature of the metal center and the other ligands, sulfur dioxide can have different modes of binding: (i) η^1 -S-planar, (ii) η^1 -S-pyramidal, (iii) η^2 -S,O-side-bound, (iv) η^1 -O-linear, (v)

η^1 -O-bent in a *U*- or *Z*-configuration, (vi) η^2 -O,O-chelate, (vii) η^3 -allyl-like.



Binding modes (i)–(iii) and (v)' have been previously observed and structurally characterized in moderately stable metal and nonmetal complexes, whereas modes (iv), (v)'', (vi), and (vii) are putative and have not yet been observed.

Despite the many binding modes of ligating SO₂, the only reported study on photoinduced SO₂ linkage isomers is by Johnson and Dew,⁶ who proposed, on the basis of low-temperature IR shifts, linkage isomerization to an η^2 binding mode of sulfur dioxide upon solid-state irradiation of *trans*-[Ru(NH₃)₄Cl(SO₂)]Cl with 365 nm light. The formation of a η^2 -S,O-bound linkage isomer was supported by ¹⁸O isotopic substitution studies. Though the IR shifts are quite similar to those observed for transition metal nitrosyl complexes,^{7,8} the

* Address correspondence to this author. Tel: (716) 645-6800 × 2217. Fax: (716) 645-6948. E-mail: coppens@acsu.buffalo.edu.

[†] State University of New York at Buffalo.

[‡] State University College of New York at Buffalo.

(1) Coppens, P.; Fomichev, D. V.; Carducci, M. D.; Culp, K. *J. Chem. Soc., Dalton Trans.* **1998**, 865–872.

(2) Coppens, P.; Novozhilova, I.; Kovalevski, A. Yu. *Chem. Rev.* **2002**, 102(4), 861–884.

(3) Kim, C. D.; Pillet, S.; Wu, G.; Fullagar, W. K.; Coppens, P. *Acta Crystallogr. A* **2002**, 58, 133–137.

(4) Ryan, R. R.; Kubas, G. J.; Moody, D. C.; Eller, P. G. *Struct. Bonding (Berlin)* **1981**, 46, 48–100. Kubas, G. J. *Acc. Chem. Res.* **1994**, 27, 182–190.

(5) Mingos, D. M. P. *Transition Met. Chem.* **1978**, 3, 1–15.

(6) Johnson, D. A.; Dew, V. C. *Inorg. Chem.* **1979**, 11, 3273–3274.

similarity between the two light-induced effects seems to have gone unnoticed at the time.

We report here on the crystallographic and spectroscopic identification of Johnson and Dew's linkage isomer and describe a related η^2 isomer of solid *trans*-[Ru(NH₃)₄(H₂O)(SO₂)](C₆H₅SO₃)₂, which differs by exhibiting longer and almost equal Ru–O(SO) and Ru–S(O₂) distances. Throughout this article we also use the notation common for the nitrosyl linkage isomers,² for which the η^2 isomer (iii for SO₂) is referred to as MS2, and the oxygen bound η^1 isomers (iv, v' and v'') as MS1.

Experimental Section

Preparation of the Ruthenium Complexes. Materials. Regular distilled water was used in all preparations. Sulfur dioxide gas, 4-trifluoromethylpyridine, triflic acid, and benzene sulfonic acid were purchased from Aldrich and used without further purification.

***trans*-Tetraaminechloro(sulfurdioxide)ruthenium(II) chloride (1).** The complex *trans*-[Ru(NH₃)₄Cl(SO₂)]Cl (**1**) was prepared from [Ru(NH₃)₅Cl]Cl₂ by the method of Wiberly et al.⁹ Crystals suitable for single-crystal X-ray analysis were obtained by recrystallization of the product from 1 M HCl by slow evaporation.

***trans*-Tetraamine(*p*-trifluoromethylpyridine)(sulfurdioxide)-ruthenium(II) triflate (2).** The complex was prepared as described for its *trans*-imidazole analogue.¹⁰ A 0.05 g (0.164 mmol) portion of **1** was mixed with 0.12 mL (0.164 mmol) of *p*-trifluoromethylpyridine in 3.5 mL of hot water. The resulting mixture was stirred until complete mixing upon which the solution became yellow-brown (~10 min). After filtering, 3.5 mL of 3 M HOTf (triflic acid) was added to give an immediate crystalline yellow-orange precipitate, which was allowed to stand overnight in a refrigerator. The crystals were collected on a glass frit, washed with diethyl ether, and air-dried to yield 0.08 g (70% yield) of **2**.

***trans*-Tetraaminoquo(sulfur dioxide)ruthenium(II) benzene sulfonate (3). Method A.** Benzene sulfonic acid (3 mL) and 7 mL of water were added to 0.05 g (0.070 mmol) of **2**. The mixture was heated and stirred until all of the starting material was dissolved to give a clear solution. After 2 weeks at room temperature, yellow-orange crystals suitable for X-ray analysis formed. They were filtered, washed with Et₂O, and air-dried to give an almost quantitative yield of *trans*-[Ru(NH₃)₄(H₂O)(SO₂)](C₆H₅SO₃)₂ (**3**). **Method B.** A 0.2 g portion of freshly prepared *trans*-[Ru(NH₃)₄(HSO₃)₂]Cl, an intermediate in the preparation of *trans*-[Ru(NH₃)₄Cl(SO₂)]Cl (**1**), was dissolved at 60 °C in a minimum volume (10–15 mL) of 20% benzene sulfonic acid. The solution was stirred for 30 min, filtered while still hot, and left in a refrigerator overnight, during which the product crystallized as yellow-orange bricks. They were collected by filtration, washed with ethanol and diethyl ether, and air-dried to yield 0.155 g of **3** (60%). Crystals suitable for X-ray analysis were obtained by recrystallization of the material from 30% benzene sulfonic acid. The crystals obtained with the two methods gave identical diffraction patterns.

Photocrystallography. X-ray diffraction data on **1** and **3** were collected at 90(1) K using a Bruker SMART1000 CCD diffractometer installed at a rotating anode source (Mo K α radiation) and equipped with an Oxford Cryosystems nitrogen gas-flow apparatus. The data were collected by the rotation method with 0.3° frame-width (ω scan) and 20 s exposure time per frame. For each experiment four sets of data (600 frames in each set) were collected, nominally covering half of the reciprocal space. The data were integrated, scaled, sorted, and

averaged using the SMART software package.¹¹ The structures were solved by the Patterson method using SHELXTL NT version 5.10.¹²

Crystals mounted in situ on the diffractometer and cooled to 90 K were irradiated with 488 nm light from Ar⁺ CW laser. The crystals were continuously rotated around the diffractometer φ angle (at 5 min/360° rotation rate) to maximize uniformity of irradiation. The laser output power was reduced to 0.5 W to minimize damage to the crystals. A crystal of **1** was irradiated for 2 h during which it darkened from bright orange-brown to deep brown. A crystal of **3** was irradiated in the same way, but with an exposure time of only 10 min as the Bragg spots weakened and a powder pattern appeared on further irradiation. In both cases data collection was started after a delay of 10–20 min in order to dissipate any heat accumulated in the crystal during light exposure.

Irradiation at 90 K of a single crystal of **1** with either a 325 nm He–Cd CW laser or a 355 nm Nd:YAG pulsed laser destroyed the crystals in a matter of seconds as indicated by the appearance of a strong powder pattern.

To minimize systematic errors, in both cases “DARK” (before irradiation) and “LIGHT” (after irradiation) data were collected on the same crystal. Identical collection and integration procedures were used. Crystallographic data for compounds **1** and **3** are presented in Table 1.

Differential Scanning Calorimetry (DSC). A Perkin-Elmer differential scanning calorimeter DSC7 was used for the DSC experiments. To maintain good temperature control the sample cavity was continuously purged with ultrapure He gas. To minimize moisture in the system the cold reservoir was flushed with N₂ gas. After at least 30 min of exposure of 5–10 mg crystalline samples to 488 nm light from an Ar⁺ laser and a delay of 10–20 min for thermal equilibration, the samples were heated at a constant rate of 4°/min starting from 100 K, as the enthalpy supplied for the heating was being monitored.

Infrared Spectroscopy. FT-IR experiments were performed on a BioRad FTS40A IR spectrometer equipped with an MCT detector. An APD Helitran LT-3-110 optical cryostat equipped with NaCl windows and connected to a liquid nitrogen tank was used to cool the samples to 90 K. Freshly prepared KBr pellets (approximately 1 mm thick) were mounted in an IR transmission cell equipped with NaCl windows. The cell was mounted in the cryostat and evacuated to approximately 10^{–7} bar using a turbomolecular pump. The temperature of the sample was controlled to within 1 K using a Scientific Instruments temperature controller (9620-R-1-1). The sample was irradiated in situ at 90 K for approximately 15–20 min with light from a 300 W Xe arc lamp passed through a heat absorbing water filter and a 350–550 nm broadband filter. Samples were mounted at 45° to both the IR beam and the irradiating beam. Spectral resolution was 1 cm^{–1}.

To obtain kinetic data on the decay of the metastable species, IR spectra of the irradiated samples were measured as a function of time at different temperatures. After irradiation, each sample was warmed to the selected temperature and 7–10 spectra were collected at fixed time intervals. Temperature ranges of 215–240 K and 235–270 K with 5 K steps were used for compounds **1** and **3**, respectively.

Plots of the natural logarithm of the maximum absorbance vs time at each temperature are linear, indicating first-order kinetics of the MS2-to-GS thermal back-reaction and allowing determination of the rate constant *k*. Plots of ln *k* vs 1/*T* for compounds **1** and **3** are shown in Figure 1 and discussed further below.

Theoretical Calculations. All calculations were performed with the GAUSSIAN98 package¹³ using Density Functional Theory with the local density approximation (LDA) in the parametrization of Vosko, Wilk, and Nusair (VWN5).¹⁴ Two different basis sets were employed. Basis set 1 consisted of a triple- ζ 6-311++G** set for N, O, S, Cl, and H atoms and a double- ζ Effective Core Potential (ECP) LANL2DZ

(7) (a) Hauser, U.; Oestreich, V.; Rohrweck, H. D. *Z. Physik A* **1977**, *280*, 17–25. (b) Hauser, U.; Oestreich, V.; Rohrweck, H. D. *Z. Physik A* **1977**, *280*, 125–30.

(8) Crichton, O.; Rest, A. *J. Chem. Soc., Dalton Trans.* **1977**, 986–993.

(9) Vogt, L. H., Jr.; Katz, J. L.; Wiberly, S. *Inorg. Chem.* **1965**, *4*, 1157–1160.

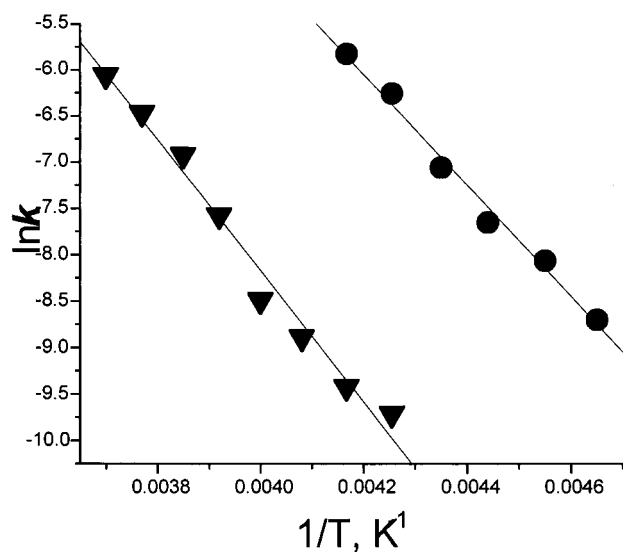
(10) Brown, G. M.; Sutton, J. E.; Taube, H. *J. Am. Chem. Soc.* **1978**, *100*, 2767–2773.

(11) SMART and SAINTPLUS, ver. 6.01; area detector control and integration software; Bruker AXS: Madison, WI, 1999.

(12) SHELXTL, v5.10; integrated system for solving, refining and displaying crystal structures from diffraction data; Bruker AXS: Madison, WI, 1997.

Table 1. Crystallographic Data for **1** and **3** at 90 K

	1		3	
	GS	MS2/GS	GS	MS2/GS
crystal color/shape	orange-brown bricks	deep brown bricks	yellow-orange bricks	deep red bricks
crystal system	orthorhombic	orthorhombic	triclinic	triclinic
space group	<i>Pnma</i>	<i>Pnma</i>	<i>P1</i>	<i>P1</i>
<i>a</i> [Å]	13.886(2)	13.8336(8)	7.0137(2)	7.0244(2)
<i>b</i> [Å]	7.2451(9)	7.2918(4)	12.8351(4)	12.8381(3)
<i>c</i> [Å]	9.246(1)	9.2037(6)	12.9606(4)	13.0303(3)
α [deg]	90	90	111.327(1)	111.581(1)
β [deg]	90	90	90.387(1)	90.336(1)
γ [deg]	90	90	101.198(1)	101.447(1)
<i>V</i> [Å ³]	930.2(2)	928.4(1)	1062.31(6)	1066.95(5)
<i>Z</i>	4	4	2	2
ρ_{calc} [g/cm ³]	2.172	2.176	1.768	1.761
μ [mm ⁻¹]	2.442	2.447	1.084	1.080
<i>T</i> [K]	90.0(1)	90.0(1)	90.0(1)	90.0(1)
max 2θ [deg]	60.1	60.1	60.1	60.1
absorption correction method	face-indexed	face-indexed	SADABS ⁹	SADABS ⁹
reflections measured	13678	15219	19296	19133
unique reflections (<i>R</i> _{int})	1467 (0.098)	1458 (0.079)	6197 (0.070)	6210 (0.060)
reflections <i>I</i> > 4 σ (<i>I</i>)	1180	1210	5425	5237
<i>R</i> ₁ [<i>I</i> > 2 σ (<i>I</i>)]	0.035	0.030	0.035	0.041
w <i>R</i> ₂	0.073	0.070	0.075	0.093
GOF	1.278	1.286	1.149	1.333

**Figure 1.** Arrhenius plots for compounds **1** (●) and **3** (▼). The solid lines show linear fits to the experimental points.

set for the ruthenium atom. In basis set 2 an extended triple- ζ 6-311++G(2df,2pd) basis set was used for the N, O, S, and Cl atoms and a 6-31+G** set for the H atoms. The Ru atom was treated as in set 1. All molecular geometries were optimized without symmetry restrictions. Convergence criteria of 10^{-6} (au) for the density matrix, 4.5×10^{-4} (au/Å) for the gradients and 1.8×10^{-3} (Å) for the displacements were used. All calculations were spin-restricted.

- (13) Frisch, M. J.; Trucks, G. W.; Schlegel, H. B.; Scuseria, G. E.; Robb, M. A.; Cheeseman, J. R.; Zakrzewski, V. G.; Montgomery, J. A.; Stratmann, R. E.; Burant, J. C.; Dapprich, S.; Millam, J. M.; Daniels, A. D.; Kudin, K. N.; Strain, M. C.; Farkas, O.; Tomasi, J.; Barone, V.; Cossi, M.; Cammi, R.; Mennucci, B.; Pomelli, C.; Adamo, C.; Clifford, S.; Ochterski, J.; Petersson, G. A.; Ayala, P. Y.; Cui, Q.; Morokuma, K.; Malick, D. K.; Rabuck, A. D.; Raghavachari, K.; Foresman, J. B.; Cioslowski, J.; Ortiz, J. V.; Stefanov, B. B.; Liu, G.; Liashenko, A.; Piskorz, P.; Komaromi, I.; Gomperts, R.; Martin, R. L.; Fox, D. J.; Keith, T.; Al-Laham, M. A.; Peng, C. Y.; Nanayakkara, A.; Gonzalez, C.; Challacombe, M.; Gill, P. M. W.; Johnson, B. G.; Chen, W.; Wong, M. W.; Andres, J. L.; Head-Gordon, M.; Replogle, E. S.; Pople, J. A. *GAUSSIAN98*; Gaussian, Inc.: Pittsburgh, PA, 1998.
- (14) Vosko, S. H.; Wilk, L.; Nusair, M. *Can. J. Phys.* **1980**, *58*, 1200–1211.

Results

GS Structure of 1. The ground-state structure was refined by full-matrix least-squares with anisotropic temperature parameters for all non-hydrogen atoms. Hydrogen atoms were located in the difference Fourier maps and placed in idealized positions 0.90 Å from the corresponding N atom and assigned $U_{\text{iso}} = 1.5U_{\text{eq}}$ of the nitrogen atom. The NH₃ groups were allowed to rotate around the N–Ru bonds during the refinement. Final agreement factors are $R_1 = 0.035$, $wR_2 = 0.073$. Final positional and isotropic temperature parameters and anisotropic displacement parameters are listed in Tables S1 and S2 (see Supporting Information), while bond lengths and angles are given in Table S4. The molecular structure is illustrated in Figure 2.

DSC Experiment and MS2 Structure of 1. The dark-light difference DSC curve of irradiated crystals of *trans*-[Ru(NH₃)₄-Cl(SO₂)Cl], is shown in Figure 3a. The light-induced metastable state shows the maximal decay rate at 257 K.

In the initial refinement all atoms were located at the ground-state positions. The fractional coordinates of the GS structure were adjusted to account for slight differences between the unit cell dimensions from the “dark” and “light” experiments, such that the geometry of the GS molecule was as in the GS structure. Refinement of only the scale factor yielded the agreement factors $R_1 = 0.056$, $wR_2 = 0.143$. Photodifference maps using the scale factor from the refinement (Figure 4) showed several light-induced residual features, ranging from a maximum of $4.9 \text{ e}/\text{Å}^3$ to a minimum of $-5.8 \text{ e}/\text{Å}^3$, 0.31 Å from the position of the Ru atom and 0.06 Å from the position of S atom, respectively. Similar but smaller features are found near the other atoms of the cation. The pattern of the light-induced peaks is in agreement with a η^1 -S-planar-to- η^2 -S,O-side-bound linkage isomerization of the sulfur dioxide ligand. The second oxygen of the SO₂ group is no longer located in the mirror plane and thus disordered over two equally occupied, mirror-plane related, positions (Figure 4c).

The subsequent least-squares refinement of the metastable state MS2 was carried out as described in detail for the nitrosyl

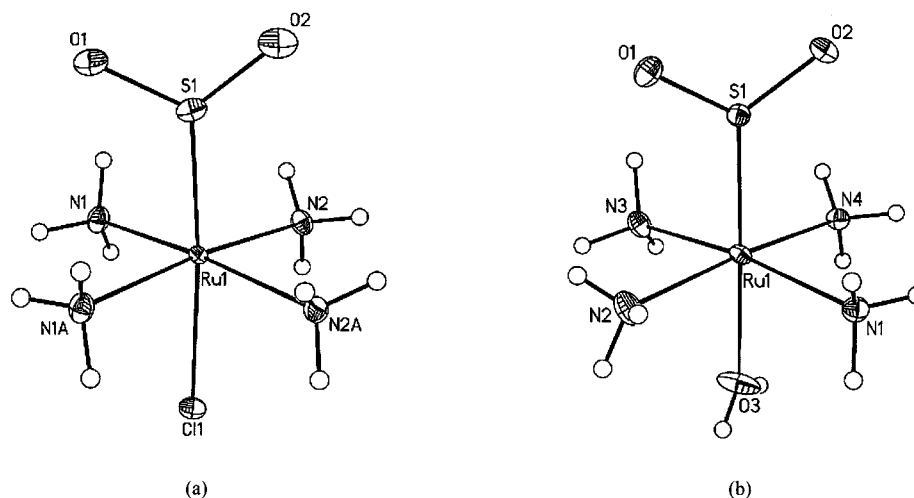
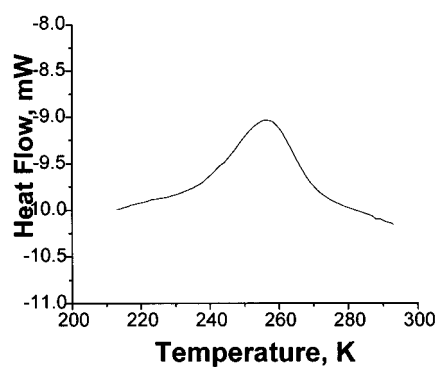


Figure 2. Geometry of the cation of **1** (a) and of **3** (b) and numbering of the atoms. 50% probability ellipsoids are shown. Atoms N1A and N2A in **1** are related to N1 and N2 by the crystallographic mirror plane.



(a)

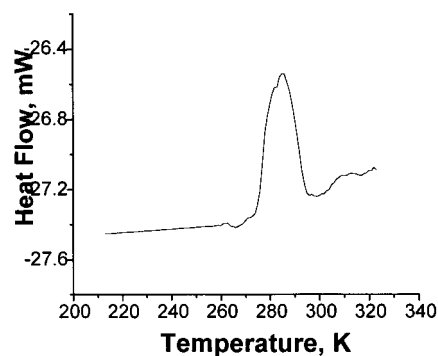


Figure 3. Heat flow vs temperature, for a constant temperature increase of 4 K/min, of a previously laser-irradiated single-crystal sample of **1** (a) and **3** (b).

transition metal complexes.^{1,15} The expression for the structure factor F of the partially converted crystal, assuming a random distribution of the metastable molecules in the crystal, is

$$F = (1 - P)F_{\text{GS}} + PF_{\text{MS}} + F_{\text{rest}}$$

where GS and MS indicate the ground and metastable states, respectively. P is the metastable state population, while the subscript “rest” represents any component of the crystal not involved in the excitation.

(15) Fomitchev, D. V.; Coppens, P. *Inorg. Chem.* **1996**, *35*, 7021–7026.

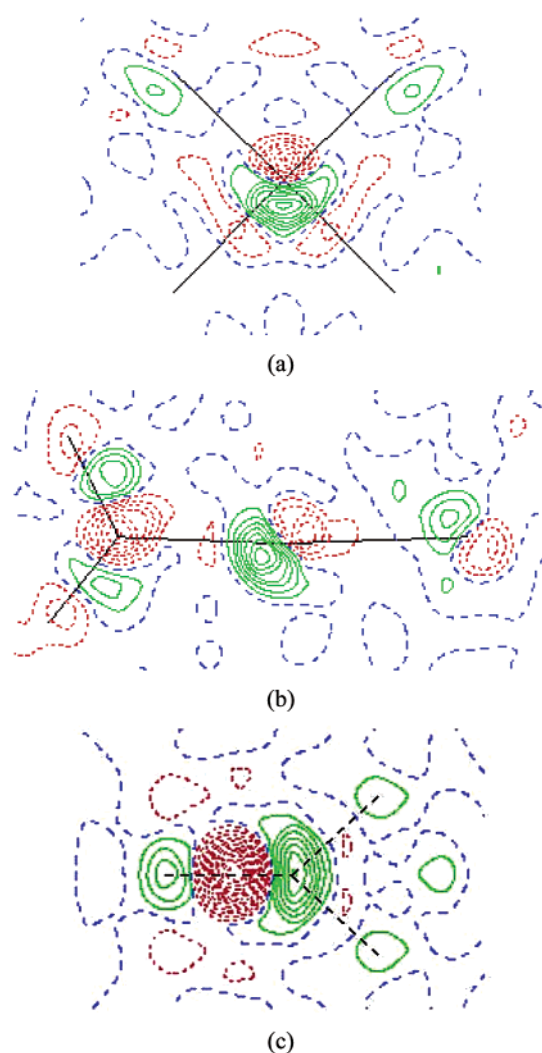


Figure 4. Photodifference Fourier maps of **1**: (a) 0.2 Å above the plane of the equatorial ligands, (b) in the crystallographic mirror plane, (c) 2.2 Å above the equatorial plane. Contour levels are at 0.4 e/Å³ for (a) and (c) and 0.8 e/Å³ for (b); negative contours are dotted and positive are solid. Black solid lines represent the GS structure connectivity, while black dashed lines in (c) show connectivity in the disordered η^2 -SO₂ ligand.

The population of MS2 and its atomic coordinates were refined starting with the coordinates deduced from the photo-

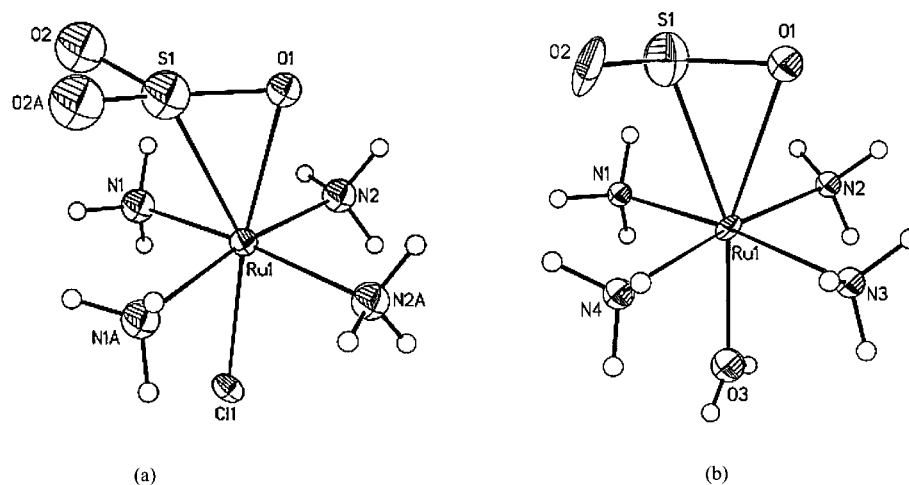


Figure 5. Geometry of the cation of **1** (a) and **3** (b) in the metastable state MS2 and numbering of atoms. 50% probability ellipsoids are shown. Atoms N1A, N2A, and O2A of **1** are related by the crystallographic mirror plane to N1, N2, and O2, respectively.

difference maps. Isotropic thermal parameters of the MS2 atoms were kept equal to the corresponding U_{eq} values of GS. The MS2 population refined to 10.0(1)%. In a subsequent stage, the GS molecule was treated as a rigid body and allowed all possible translations and rotations. Only minor changes from the ground-state structure occurred; atomic shifts did not exceed 0.001 Å. Positional and thermal parameters of the anion were also varied in this refinement. In the final stage, positional and isotropic thermal parameters of MS2 (anisotropic for Ru and Cl atoms) were also refined to give $R_1 = 0.030$ and $wR_2 = 0.070$. The highest remaining maximum and deepest minimum in the difference Fourier synthesis were 0.78 and $-1.73 \text{ e}/\text{Å}^3$, respectively. Final positional and thermal parameters of the MS2 structure are listed in Table S3. The bond lengths and angles of the MS2 structure are given in Table S4, and the geometry of the MS2 molecule is illustrated in Figure 5a.

GS Structure of 3. The ground-state structure (Figure 2) was refined by full-matrix least-squares with anisotropic temperature parameters for all non-hydrogen atoms to give final agreement factors $R_1 = 0.035$, $wR_2 = 0.075$. Amine hydrogen atoms were treated as in the structure analysis of **1**. Hydrogen atoms of the water molecule were refined independently with U_{iso} fixed at $1.5U_{eq}$ of the O atom. Final positional and isotropic temperature parameters and anisotropic displacement parameters are listed in Tables S5 and S6, and bond lengths and angles are presented in Table S8.

DSC Experiment and MS2 Structure of 3. The difference DSC curve for *trans*-[Ru(NH₃)₄(H₂O)(SO₂)](C₆H₅SO₃)₂ is shown in Figure 3b. The metastable state shows the maximal decay rate at 282 K.

The refinement of the structure was performed as described for **1**. Starting positions for all atoms were taken from the ground-state structure. Refinement of the scale factor only gave the agreement factors $R_1 = 0.084$, $wR_2 = 0.222$. Subsequent photodifference maps showed new residual features, ranging from a maximum of $11.7 \text{ e}/\text{Å}^3$ to a minimum of $-4.8 \text{ e}/\text{Å}^3$, 0.40 and 0.22 Å from the position of the Ru atom, respectively (Figure 6a and 6b). As in **1**, the electron density peaks indicate a photoinduced η^1 -S-planar-to- η^2 -S,O-side-bound linkage isomerization of the sulfur dioxide ligand with, in this case, a fully ordered side-bound SO₂ (Figure 6c).

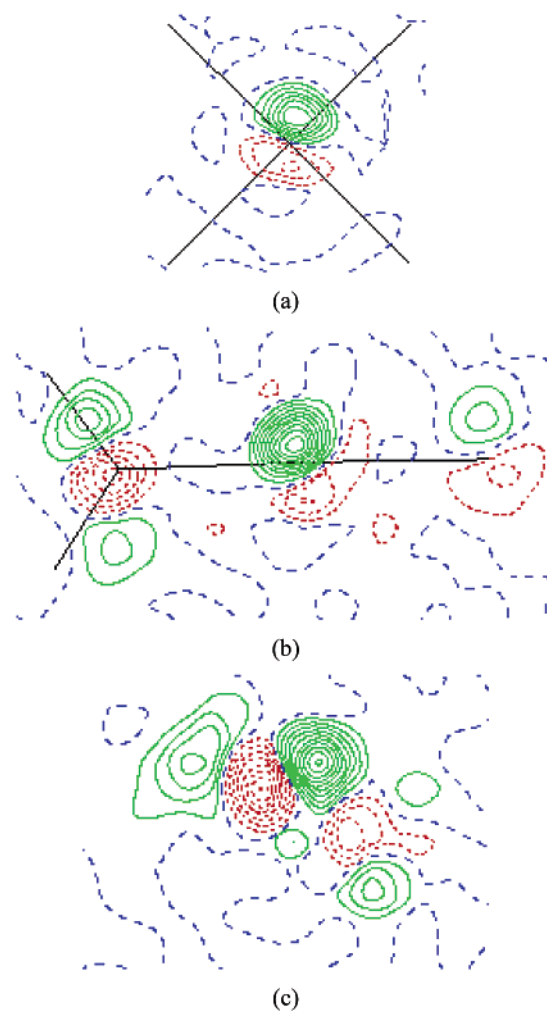


Figure 6. Photodifference Fourier map of **3** in different planes: (a) 0.1 Å above the equatorial plane with the Ru1 atom at the center; (b) in a plane containing O3, Ru1, and SO₂; (c) 2.4 Å above the equatorial plane. Contour levels are at (a) $1.6 \text{ e}/\text{Å}^3$, (b) $0.8 \text{ e}/\text{Å}^3$, (c) $0.4 \text{ e}/\text{Å}^3$; negative contours are dotted and positive are solid. Black solid lines represent the GS structure connectivity.

In the final stage, positional and isotropic thermal parameters of MS2 (anisotropic for the Ru, S, and O2 atoms) were refined to give $R_1 = 0.041$ and $wR_2 = 0.093$. The MS2 population

refined to 11.1(1)%. The highest remaining peak and deepest minimum in the difference Fourier synthesis are 1.39 and -2.32 $e/\text{\AA}^3$, respectively. Final positional and thermal parameters of the MS2 structure are listed in Table S7, and the bond lengths and angles are summarized in Table S8. The geometry of MS2 molecule is illustrated in Figure 5b.

Discussion

Geometry of the Light-Induced Metastable States. (Figure 6; see Supporting Information for a discussion of the ground state geometries.) Although complexes with the η^2 -S,O-side-bound sulfur dioxide geometry are known,^{16,17} including those of Ru(0),^{18,19} no structures of η^2 -S,O-side-bound SO₂ complexes of Ru(II) have been reported.

Geometry changes upon transition to the metastable state of **1** are analogous to those observed for metal-nitrosyl MS2 isomers,^{20,21} including shortening of the bond between Ru and the trans-to-SO₂ axial ligand and a change in the umbrella-like conformation of the equatorial ligands. The Ru–Cl bond is shortened by 0.085(11) \AA , while the ruthenium atom is displaced from the plane of amine nitrogen atoms by 0.150 \AA toward the SO₂ ligand in MS2, compared with 0.105 \AA in GS. In contrast, in **3** the axial bond length from the water oxygen to the ruthenium atom shortens only slightly from 2.101(2) \AA in GS to 2.08(2) \AA in MS2, and the displacement of Ru from the plane of the equatorial ligands is almost identical in both states (GS: 0.122 \AA , MS2 0.110 \AA). The Ru–N distances are not changed within experimental errors in both compounds. In **1** the S1 and O1 atoms that are bound to the Ru atom are located in the mirror plane, but O2 is displaced from the mirror plane and thus distributed over two positions. The S1–O1 and S1–O2 bond lengths, though not accurately determined, are in good agreement with those reported for stable side-bound Rh and Mo SO₂ complexes.^{22,23} As is the case for other η^2 -SO₂-bound transition metal complexes, the sulfur dioxide plane is not parallel to the plane of the equatorial nitrogen atoms but inclined by 21° in **1** and 13° in **3**.

The O1 oxygen atom in **1** is much closer to the Ru than the sulfur atom and is located close to the molecular axis, while the S atom is displaced from the axis toward N, the S1–Ru–Cl angle being 150.1(5)°. However, the experimental Ru–S1 and Ru–O1 distances in **3** are almost equal to each other but longer by 0.19 and 0.08 \AA , respectively, than the same bonds in **1** (Table 3). The S1–Ru–O3(water) and O1–Ru–O3(water) bond angles are identical at $\sim 161^\circ$ (Figure 5). As in **1**, the S1–O1 bond coordinated to Ru is in an almost *staggered* orientation with the respect to two N–Ru bonds (the torsion angle O1–S1–Ru–N3 is 39.2(8)°).

For both **1** and **3** small changes in the cell dimensions (up to 0.5% and not larger than 0.07 \AA) are observed upon irradiation (Table 1). The expansion occurs along the y axis in **1** and along

Table 2. Selected Experimental and Theoretical Bond Lengths (\AA), Angles (deg), and Frequencies (cm^{-1}) for the *trans*-Ru(NH₃)₄(SO₂)Cl⁺ Cation (**1**)

	experiment		theory					
			basis set 1			basis set 2		
	GS	MS2	GS	MS2	MS1	GS	MS2	MS1
Ru1–S1(O ₂)	2.080(1)	2.32(2)	2.137	2.424		2.114	2.373	
Ru1–O1(SO)		2.19(3)		2.130	1.973		2.124	1.981
Ru1–Cl1(tr)	2.407(1)	2.32(1)	2.346	2.311	2.312	2.338	2.297	2.293
Ru1–N(eq)	2.110(2)	2.08(3)	2.105	2.097	2.102	2.105	2.099	2.102
	2.110(2)	2.08(3)	2.105	2.091	2.104	2.105	2.099	2.102
	2.113(2)	2.09(3)	2.106	2.115	2.103	2.108	2.115	2.102
	2.113(2)	2.09(3)	2.106	2.100	2.102	2.108	2.101	2.102
S1–O1	1.451(3)	1.46(3)	1.478	1.565	1.553	1.457	1.534	1.523
S1–O2	1.426(4)	1.41(6)	1.468	1.490	1.499	1.457	1.473	1.479
∠OSO	114.8(2)	138(3)	118.5	114.3	111.0	117.8	114.4	112.0
∠NRuSO	44.55(7)	49.3(8)	43.9	44.7	42.8	–23.4	42.3	42.9
$\nu_{\text{symm}}(\text{SO})$	1110	942	1080	887	856	1120	943	910
$\nu_{\text{asymm}}(\text{SO})$	1253	1165	1264	1126	1101	1301	1163	1150

Table 3. Selected Theoretical Bond Lengths (\AA), Angles (deg), and Frequencies (cm^{-1}) for the *trans*-Ru(NH₃)₄(SO₂)(H₂O)²⁺ Cation (**3**)

	experiment		theory					
			basis set 1			basis set 2		
	GS	MS2	GS	MS2	MS1	GS	MS2	MS1
Ru1–S1(O ₂)	2.0853(4)	2.41(1)	2.127	2.476		2.104	2.414	
Ru1–O1(SO)		2.38(2)		2.076	1.952		2.063	1.954
Ru1–O3(tr)	2.101(2)	2.08(2)	2.154	2.092	2.103	2.162	2.098	2.098
Ru1–N(eq)	2.123(2)	2.17(2)	2.129	2.133	2.124	2.126	2.132	2.119
	2.114(2)	2.10(2)	2.115	2.106	2.115	2.113	2.104	2.114
	2.121(2)	2.11(2)	2.129	2.124	2.110	2.127	2.121	2.109
	2.117(2)	2.11(2)	2.115	2.112	2.107	2.115	2.112	2.105
S1–O1	1.446(1)	1.51(2)	1.462	1.571	1.549	1.447	1.543	1.524
S1–O2	1.448(1)	1.45(2)	1.462	1.476	1.478	1.446	1.459	1.461
∠OSO	115.71(9)	118(1)	121.4	113.9	111.7	120.2	114.2	112.8
∠NRuSO	–26.98(8)	39.2(8)	–17.2	33.7	–7.2	12.8	26.8	–6.4
$\nu_{\text{symm}}(\text{SO})$	1126	946	1100	882	899	1140	934	945
$\nu_{\text{asymm}}(\text{SO})$	1279	1181	1286	1175	1163	1281	1208	1206

z in **3**. In both cases these are directions perpendicular to the long axis of the cation, as may be expected given the geometry change of the cation described above.

Infrared Spectroscopy. The IR spectra of *trans*-[Ru(NH₃)Cl(SO₂)]Cl are essentially the same as those reported by Johnson and Dew (JD).⁶ In the ground state bands are located at 1110 and 1253 cm^{-1} (compared with values of 1110 and 1255 cm^{-1} reported by JD), corresponding to the symmetric and antisymmetric S–O stretching vibrations, respectively. Photolysis at 90 K of the KBr pellets causes a decrease in the intensity of these bands, while bands corresponding to η^2 -side-bound SO₂ ligand of MS2 appear at 942 and 1165 cm^{-1} (JD, 940 and 1165 cm^{-1}). The corresponding bands for *trans*-[Ru(NH₃)(H₂O)(SO₂)](C₆H₅SO₃)₂ (**3**) are at 1126 and 1279 cm^{-1} for GS and at 946 and 1181 cm^{-1} for MS2.

MS2-to-GS decay rate constants at different temperatures are listed in Table 4. For **1** they were calculated from the intensities of both the symmetric and antisymmetric stretching vibrations of SO₂ and then averaged for each temperature. However, in **3** the antisymmetric S–O stretching vibration of MS2 is almost buried in the SO₃ stretching bands of the benzene sulfonate counterion, so that only the symmetric mode could be used for the determination of the rate constant. Morioka et al.²⁴ define

(24) Morioka, Y.; Ishikawa, A.; Tomizawa, H.; Miki, E. *J. Chem. Soc., Dalton Trans.* **2000**, 781–786.

(16) Baumann, F. E.; Burschka, C.; Schenk, W. A. *Z. Naturforsch., B: Chem. Sci.* **1986**, *41*, 1211–1218.

(17) Cotton, F. A.; Schmid, G. *Inorg. Chem.* **1997**, *36*, 2267–2278.

(18) Wilson, R. D.; Ibers, J. A. *Inorg. Chem.* **1978**, *17*, 2134–2138.

(19) Moody, D. C.; Ryan, R. R. *J. Chem. Soc., Chem. Commun.* **1980**, 1230–1231.

(20) Fomitchev, D. V.; Furlani, T. R.; Coppens, P. *Inorg. Chem.* **1998**, *37*, 1519–1526.

(21) Fomitchev, D. V.; Coppens, P. *Comments Inorg. Chem.* **1999**, *21*, 131–148.

(22) Kubas, G. J.; Ryan, R. R.; McCarty, V. *Inorg. Chem.* **1980**, *19*, 3003–3007.

(23) Moody, D. C.; Ryan, R. R. *Inorg. Chem.* **1977**, *16*, 2473–2478.

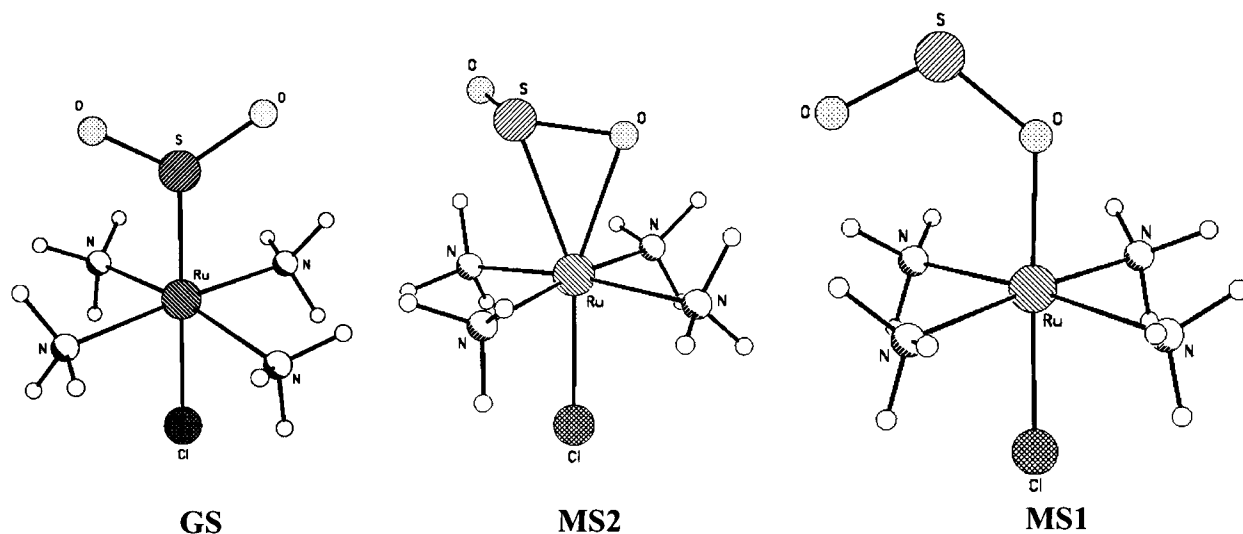


Figure 7. Theoretical conformations of the ground state (GS) and the two linkage isomers of **1** calculated using basis set 2.

Table 4. MS2 Decay Rate Constants for Compounds **1** and **3** from IR Data

1		3	
<i>T</i> (K)	<i>k</i> ^a (10 ⁻³ , s ⁻¹)	<i>T</i> (K)	<i>k</i> ^b (10 ⁻³ , s ⁻¹)
		235	0.061
		240	0.081
215	0.167	245	0.138
220	0.315	250	0.206
225	0.476	255	0.514
230	0.860	260	0.988
235	1.920	265	1.550
240	2.960	270	2.340

^a Decay constant averaged from the data of both symmetric and antisymmetric S–O vibrations. ^b Decay constant calculated using only the symmetric S–O vibration.

the decay temperature (*T*_d) as the temperature at which the rate constant for the thermal decay of the light-induced species is 10⁻³ s⁻¹. Using this definition, *T*_d of *trans*-[Ru(NH₃)Cl(SO₂)]Cl was found to be 230 K and that of *trans*-[Ru(NH₃)(H₂O)(SO₂)](C₆H₅SO₃)₂ was 262 K, compared with the maxima in the 4°/min DSC heating curves of 257 and 282 K.

The molar activation energies (*E*_a) of MS2-to-GS thermal decay reactions were derived with the Arrhenius equation:

$$\ln k = -(E_a/RT) + \text{constant}$$

where *k* is the rate constant of the reaction at the temperature *T*, and *R* is the molar gas constant. Figure 1 shows the Arrhenius plots for compounds **1** and **3**. The activation energies are found to be 50.0 kJ/mol (0.518 eV) for **1** and 58.4 kJ/mol (0.605 eV) for **3**. The higher *E*_a for **3** is in agreement with its higher decay temperature. These values may be compared with activation energies for nitrosyl linkage isomers determined by DSC and IR measurements. Using DSC, Zöllner et al. obtained the following *E*_a values for the thermal back reactions of MS1 and MS2, respectively: for sodium nitroprusside (SNP), ~0.69 and 0.50 eV;²⁵ for K₂[RuCl₅NO], 0.71 and 0.47 eV;²⁶ for K₂[Ru(NO₂)(OH)(NO)], 0.65 and 0.47 eV.²⁷ Morioka et al.,²⁴ using

IR, reported *E*_a values of the MS1-to-GS thermal back-reaction of *cis*-[Ru(Hox)(en)₂NO]Cl₂·EtOH (*T*_d = 226 K) and *trans*-[Ru(Hox)(en)₂NO]Cl₂ (*T*_d = 277 K) to be 51.5 kJ/mol (0.533 eV) and 64.4 kJ/mol (0.670 eV), respectively. Thus, the activation energies of 0.518 and 0.605 eV for the back-reaction of the MS2 isomers with the larger SO₂ ligand are slightly above the 0.47–0.50 eV range reported for the MS2 nitrosyl linkage isomers.

Theoretical Calculations on the Ground and Metastable States of [Ru(NH₃)₄(SO₂)Cl]¹⁺ (1**) and [Ru(NH₃)₄(SO₂)(H₂O)]²⁺ (**3**).** The calculations indicate that not only MS2 but also an MS1-type isomer (type (v)', *O*-bound, *U*-shaped) correspond to local minima on the potential energy surface. Although the MS1 isomer has not been observed either spectroscopically or by crystallographic methods, theory gives a reasonable geometry of this metastable state.

[Ru(NH₃)₄(SO₂)Cl]¹⁺ (1**).** Although with basis set 1 MS2 has an energy only slightly higher (+0.04 eV) than that of the GS and MS1 is somewhat less stable (+0.19 eV), with the larger set 2 MS2 is located 0.14 eV above the ground state and MS1 is much less stable (+0.55 eV), in better agreement with this species not having been observed experimentally. Although a stationary point with an energy +0.77 eV higher than that of the GS was found for a linkage isomer with the (v)'' (*Z*-configuration) structure, one of its frequencies is imaginary with an absolute value of 16 cm⁻¹.

Theoretical geometries of the GS, MS2, and MS1 linkage isomers are shown in Figure 7 and described in Table 2. The ground state geometry is reasonably well reproduced by the calculation, the best agreement being obtained with the large basis set 2, though the Ru–Cl (trans) bond distance is underestimated even with the larger basis set. The conformation of the SO₂ ligand plane with the respect to the equatorial ligands is *gauche*-like with basis set 2 (Table 2) but close to staggered with set 1, as observed experimentally. For MS2, both calculations correctly predict the Ru–S distance to be longer than Ru–O, and the Ru–Cl distance to be shorter than in GS. Both S–O bonds are elongated, in agreement with the decrease in SO stretching frequencies. The calculated IR frequencies for MS1 are very close to those of MS2, which could have masked their

(25) Zöllner, H.; Woike, T.; Krasser, W.; Haussühl, S. *Z. Kristallogr.* **1989**, *188*, 139–153.

(26) Woike, T.; Zöllner, H.; Krasser, W.; Haussühl, S. *Solid State Commun.* **1990**, *73*, 149–152.

(27) Woike, T.; Haussühl, S. *Solid State Commun.* **1993**, *86*, 333–337.

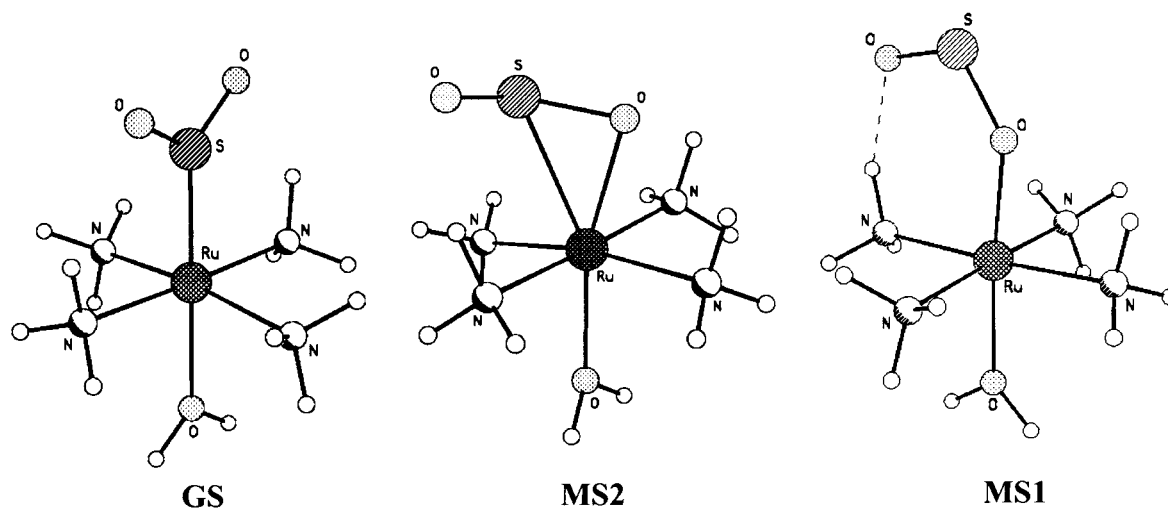


Figure 8. Theoretical conformations of the ground state (GS) and the two linkage isomers of **3** calculated using basis set 2.

occurrence in the IR spectra, though no second light-induced species was observed in the DSC experiments.

[Ru(NH₃)₄(SO₂)(H₂O)]²⁺ (3**).** As for cation **1**, basis set 1 gives an energy of MS2 only slightly above (+0.03 eV) that of GS, while MS1 is predicted to be more stable than the ground state, its energy being *lower* by −0.17 eV than that of GS, a result that contradicts this species not having been observed. With basis set 2 the MS2 energy is considerably higher (+0.27 eV), whereas MS1 is slightly more stable than MS2 (+0.24 eV). The stabilization of the MS1 isomer results from an intramolecular hydrogen bond between the distal oxygen atom of sulfur dioxide and one of the amine hydrogen atoms. Figure 8 shows the optimized theoretical geometries of all three linkage isomers, with the hydrogen bond in MS1 indicated by a dashed line. Numerical details are given in Table 3. Basis set 2 reproduces the geometry of GS well, with the exception of the Ru–O and Ru–S distances to the η²-bound SO₂ in the MS2, which are quite different, rather than virtually identical as observed in the experiment. The discrepancy between theory and experiment is pronounced for the Ru–O distance and the position of the S atom relative to the molecular axis. It is possible that this disagreement reflects the influence of the crystallographic environment on the geometry of MS2.

Unlike for **1**, MS1 of **3** is calculated to have an eclipsed orientation of the SO₂ plane with respect to one of the Ru–N bonds. This results in formation of a strong intramolecular hydrogen bond N–H⋯O_{distal}, with an O⋯H distance of 1.838 Å and an N–H⋯O angle of 149.7°. The (v'') linkage isomer could not be optimized; it invariably reverted to the (v') MS1 isomer, indicating the absence of a local minimum on the potential energy surface for this configuration.

Conclusion

The photoinduced linkage isomerism of two Ru–SO₂ complexes has been fully identified by a combination of crystallographic, spectroscopic, and calorimetric techniques. The linkage isomers are more stable than the corresponding NO and

N₂ complexes, as evidenced by the larger activation energies for decay and the higher decay temperatures. SO₂ is a widely recognized genotoxic and clastogenic substance and a major industrial pollutant. Its alternate binding modes and its lability are of importance for the understanding of the mechanism of its catalytic reduction to sulfur on metal surfaces.

The nature of the linkage isomers is supported by the theoretical calculations, which also predict the existence of an oxygen-bound MS1-type isomer. The experiment shows differences in detailed geometry of the Ru–SO₂ binding of the two complexes studied here, which is not reproduced by the theoretical calculations on the isolated species, indicating that solid-state effects may play a role.

The stability of the light-induced species is affected by chemical substitution²¹ and can likely be increased, as demonstrated by Morioka for the MS1 isomer of Ru-nitrosyl complexes.²⁴ Crystals of the nitrosyl linkage isomers have been proposed as high-capacity read–write storage devices, as patterns can be written and erased with light of different wavelengths and the linkage isomerization is accompanied by a significant change in the refractive index.²⁸ The physical properties of crystals containing the SO₂ linkage isomers are not yet known but warrant further investigation.

Acknowledgment. The authors would like to thank Dr. Jacqueline Cole for participation in some of the experiments. Financial support of this work by the National Science Foundation (CHE9981864) and the Petroleum Research Fund of the American Chemical Society (PRF32638AC3) is gratefully acknowledged.

Supporting Information Available: Discussion of ground state geometries and related data (CIF). This material is available free of charge via the Internet at <http://pubs.acs.org>.

JA026045C

(28) (a) Imlau, M.; Woike, T.; Schieder, R.; Rupp, R. A. *Europhys. Lett.* **2001**, *53*, 471–477. (b) Imlau, M.; Haussuhl, S.; Woike, T.; Schieder, R.; Angelov, V.; Rupp, R. A.; Schwarz, K. *Appl. Phys. B* **1999**, *68*, 877–885.